Chapter 21

Global Analysis of FRET–FLIM Data in Live Plant Cells

Sergey P. Laptenok, Joris J. Snellenburg, Christoph A. Bücherl, Kai R. Konrad, and Jan Willem Borst

Abstract

This chapter describes the procedure for globally analyzing *f*luorescence *l*ifetime *im*aging (FLIM) data for the observation and quantification of Förster resonance energy transfer (FRET) in live plant cells. The procedure is illustrated by means of a case study, for which plant protoplasts were transfected with different visible fluorescent proteins and subsequently imaged using two-photon excitation FLIM. Spatially resolved fluorescence lifetime images were obtained by application of global analysis using the program Glotaran, which is open-source and freely available software. Using this procedure it is possible to extract the fraction and distance of interacting species between, or conformational changes within proteins, from complex experimental FRET–FLIM datasets, even at low signal-to-noise ratios. In addition, the software allows excluding inherently present autofluorescence from the plant cells, which improves the accuracy of the FRET analysis. The results from the case study are presented and interpreted in the context of the current scientific understanding of these biological systems.

Key words FLIM, FRET, mTurquoise1, Global analysis, Time-resolved fluorescence, Microscopy, Glotaran

1 Introduction

Fluorescence microscopy in combination with Förster resonance energy transfer (FRET) is nowadays a widely used method for visualizing protein interactions in living cells. FRET is a process in which the excited-state energy from a fluorescent donor molecule is transferred non-radiatively to an acceptor molecule. FRET is based on very weak dipole–dipole coupling and therefore can only occur at very short intermolecular distances, typically less than 10 nm. However, by carefully selecting the FRET pair one can detect interactions over longer distances. There are several methods to visualize FRET, of which donor fluorescence lifetime imaging (FLIM) is the most straightforward one for estimating FRET efficiencies. The fluorescence lifetime is an intrinsic property of a fluorophore giving the advantage that measurements are independent of

Yves Engelborghs and Antonie J.W.G. Visser (eds.), *Fluorescence Spectroscopy and Microscopy: Methods and Protocols*, Methods in Molecular Biology, vol. 1076, DOI 10.1007/978-1-62703-649-8_21,

fluorophore concentration. Though, the fluorescence lifetime is sensitive to the immediate environment of the fluorophore, which is the basis for FRET–FLIM measurements. Typically, FRET–FLIM experiments consist of measuring donor fluorescence lifetimes in the absence (τ_D) and presence (τ_{DA}) of acceptor molecules resulting in spatially resolved, color-coded fluorescence lifetime images. Observation of a decreased donor fluorescence lifetime due to FRET is used as an indicator for molecular interactions [1].

Well-designed data analysis protocols are indispensable for accurate and quantitative analysis of FRET–FLIM data. Global analysis is a technique which offers significant advantages in terms of improved accuracy, decreased sensitivity to noise, and the possibility of combining fluorescence decay data from different measurements [2]. A fluorescence decay can often be described by single or multiple kinetic processes depending on the electronic configuration of the fluorophore and its immediate environment. With global analysis, the kinetic rate constants can be determined simultaneously for all pixels of an image, even though the relative intensity values may vary from pixel to pixel [3]. Global analysis can be used to accurately detect FRET phenomena by estimating the fluorescence lifetime of donor molecules in the absence and presence of acceptor molecules. A complicating issue is the fact that FRET systems in cell biology are not always purely homogeneous, since they can contain a population of donor molecules that cannot transfer their excitation energy, because of either unwanted photobleaching (photodestruction) of the acceptor molecules or incomplete maturation of the acceptor proteins (this is especially the case of genetically encoded visible fluorescent proteins) [4]. Therefore, average donor lifetimes do not reflect true FRET efficiencies, because they originate from a pool of interacting and noninteracting species [5, 6].

In this chapter, a step-by-step protocol is described for the procedure of analyzing FRET–FLIM data on live plant cells by means of global analysis. A complete procedure is described ranging from sample preparation to data acquisition and subsequent analysis of the acquired data. Data analysis is carried out using the open-source and freely available software program Glotaran [7]. The data analysis protocol is illustrated using a case study, for which plant protoplasts were transiently transfected with two different plasmids: one expressing the mTurquoise1 fluorescent protein only and the second expressing a mTurquoise1–mVenus fusion protein connected by a two amino acid linker. The latter is a FRET pair, where mTurquoise1 is serving as a donor and mVenus as an acceptor with a Förster radius (see below) of 5.4 nm. Descriptive screenshots at different steps of the global analysis procedure are included as a visual guide. Finally, essential parameters resulting from the analysis, as well as the final donor fluorescence lifetime images of mTurquoise1 in presence and absence of acceptor molecules, are presented.

2 Materials and Imaging Setup

2.1 Expression Vectors, Plant Protoplasts, Microscopy Features

1. mTurquoise1 (kindly provided by Prof. Th. J. W. Gadella, University of Amsterdam) and mTurquoise1–Venus (two amino acid (LN) linker) constructs were cloned into pSAT-based vector harboring the Ubiquitin 10 promoter.
2. Plant material: Rosette leaves of *Arabidopsis thaliana* plants (ecotype Columbia) grown for 4–5 weeks under long-day conditions (16 h light/8 h dark) at 22 °C.
3. Protoplast isolation and transfection protocol can be found in Bücherl et al. [8] (*see* **Note 1**).
4. Coherent Ti:Sapphire laser (Coherent Mira D900) (Coherent Inc., Santa Clara, CA).
5. Biorad Radiance 2100MP confocal system.
6. Nikon TE 300 inverted microscope (Tokyo, Japan).
7. B&H HPM-100-40 Hybrid detectors (Becker & Hickl, Germany) (*see* **Note 2**).
8. B&H SPC 730 module (Becker & Hickl, Germany).

2.2 FRET–FLIM Data Acquisition

Spatially resolved fluorescence lifetime imaging is performed on a Biorad Radiance 2100 MP system in combination with a Nikon TE 300 inverted microscope as described in Russinova et al. [9]. Two-photon excitation pulses at 860 nm are generated by a Ti-Sapphire Laser model Mira 900 (Coherent Inc.), pumped by a 5 W continuous wave solid state laser (Coherent Verdi V5), resulting in excitation pulses of 200 fs at a repetition of 76 MHz. A 60×/1.2 water immersion objective is used (*see* **Note 3**). mTurquoise1 fluorescence emission is selected by a 480DF30 band pass filter and detected by a Becker & Hickl HPM-100-40 Hybrid detector with a time resolution of 120 ps. Fluorescence images of 64 × 64 pixel size are acquired using the B&H SPC 730 module. The resolution for the analog-to-digital (ADC) converter was set to 256 channels, resulting in a channel spacing of 48 ps/channel. The average photon count rate is around 10^4 photons per second for an acquisition time of 90 s for one measurement. Measurements of single transfected protoplasts expressing mTurquoise1 represent the reference. To elucidate FRET, donor fluorescence lifetimes of the mTurquoise1–Venus fusion are determined and compared to the mTurquoise1-only samples (*see* **Note 4**).

3 Methods

3.1 FLIM Data Analysis Summary

For each pixel in a FLIM image, the fluorescence intensity is measured as a function of time. Therefore, each pixel contains a recorded fluorescence-time trace that can be considered as a separate

experiment. The time traces of all pixels are stored as a single matrix, in which each column represents the fluorescence intensity decay associated with a single pixel.

The fluorescence decay is typically well described by a sum of exponential decay components convolved with the instrumental response function (IRF), so that the time dependent fluorescence for a single pixel reads as

$$F(t) = \sum_{I}^{n_{\text{comp}}} \alpha_i \exp\left(-\frac{t}{\tau_i}\right) \otimes g(t), \tag{1}$$

where the summation is over the number of exponential fluorescence decay components n_{comp}, τ_i is the lifetime of component i, α_i is the fractional contribution of component i to the fluorescence decay, $g(t)$ is the IRF, and $\otimes$ is the convolution operator.

The basis for global analysis is the superposition principle stating that the experimental decay is composed of a linear combination of n_{comp} components. The fact that the fluorescence lifetime components are spatially invariant is crucial for global analysis of a FLIM image (*see* **Note 9**), which has been justified by Verveer and coworkers [10]. More details about global analysis on FLIM data can be found in [11].

3.2 Summary of FRET Theory

This section summarizes the concepts of fluorescence lifetimes and FRET, which can be found in textbooks on fluorescence spectroscopy [12, 13]. The fluorescence lifetime of a fluorophore τ is the average time that the molecule stays in the excited state after response to a very short excitation pulse and is given as a function of the radiative (k_{r}) and non-radiative (k_{nr}) rate constants: $\tau = 1/(k_{\text{r}} + k_{\text{nr}})$. Since the fluorescence lifetime of a fluorophore is sensitive to the local environment (e.g., pH, charge, presence of quenchers, refractive index, temperature), lifetime measurements under a microscope offer the important advantage of contrast by spatial variations of lifetimes [1]. FRET is a bimolecular process in which the excited-state energy of a donor fluorophore is nonradiatively transferred with rate constant (k_{T}) to a ground-state acceptor molecule by very weak dipole–dipole coupling. The fluorescence lifetime of donor molecules that involves FRET becomes shorter compared to donor molecules in the absence of acceptor and can be calculated using $\tau_{\text{da}} = 1/(k_{\text{r}} + k_{\text{nr}} + k_{\text{T}})$. The transfer rate constant can be calculated knowing the fluorescence lifetime of the donor in presence and absence of acceptor as

$$k_{\text{T}} = k_{\text{da}} - k_{\text{d}} = \frac{1}{\tau_{\text{da}}} - \frac{1}{\tau_{\text{d}}}. \tag{2}$$

The transfer rate (k_{T}) is proportional to the inverse 6th power of the distance r between donor and acceptor molecules, which

makes this technique an extremely sensitive parameter for obtaining distances as

$$k_T = k_d \left(\frac{R_0}{r} \right)^6, \tag{3}$$

where r is the actual distance between donor, kd is equal to $1/\tau d$ and acceptor and R_0 is the so-called critical or Förster radius [14], defining the distance between donor and acceptor at which 50 % of the donor energy is transferred to the acceptor.

The efficiency of energy transfer (E) can be obtained as

$$E = \frac{k_T}{k_d + k_T} = \frac{R_0^6}{R_0^6 + r^6}. \tag{4}$$

3.3 Software Installation and Compatibility

All experimental data described in this chapter are visualized and analyzed using the Glotaran software. Glotaran was designed to be cross-platform, so that it will run on a wide variety of different operating systems (Windows, Linux, Mac OS). Detailed system requirements, installation instructions, and installers for Glotaran can be obtained from http://www.glotaran.org (*see* **Note 5**). FLIM data need to be in the correct format before visualization or analysis. Glotaran accepts either raw data files obtained from B&H and PicoQuant photon counting cards or plain text data files that are formatted as described in [15].

3.4 Data Preprocessing

1. Once Glotaran is installed and set up as described in Subheading 3.3, the analysis can be started by first creating a *New Project* (File—New Project), where project data such as raw data, models, and analysis results are stored (*see* Fig. 1).
2. Right click on the *Datasets* folder and select "Open dataset file" to create a new data reference file. A dialog window will appear from which data files can be selected and imported (*see* **Note 6**). The data reference file will appear in the project explorer under the *Datasets* folder (*see* Fig. 1).
3. After opening a data reference file or a dataset (double click on file in project explorer), the corresponding data displayer will show the content of the opened file. The first tab of the FLIM data displayer, labeled Data (Fig. 2), displays a fluorescence intensity image (*see* **Note 7**) (Fig. 2). The pixels that are selected for analysis are shown in green, and the corresponding fluorescence decay profile of the last selected pixel is displayed in the *Selected trace* panel (Fig. 2). The sum of the fluorescence decay profiles of all selected pixels is plotted in the *Sum Trace* panel (Fig. 2). The time window can be adjusted by changing the position of the sliders (indicated below the decay profile). The selected time window appears highlighted in the *Sum*

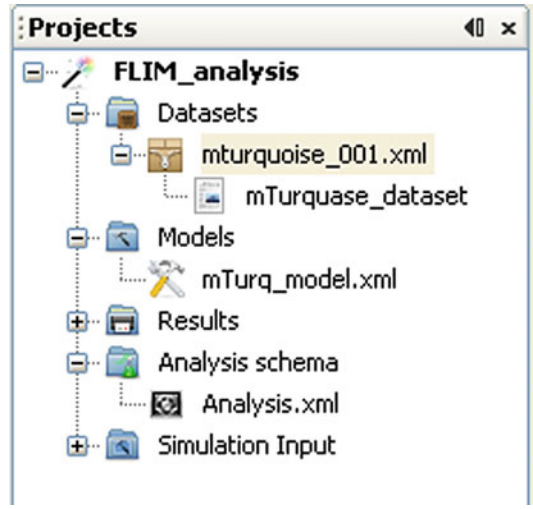

Fig. 1 Screenshot of the project manager in Glotaran. Here, "FLIM_analysis" is the opened project representing a Glotaran project folder on disk. *Datasets*, *Models*, *Results*, *Analysis schema*, and *Simulation Input* are the standard subfolders of any Glotaran project folder. The *Datasets* folder contains references to data files (here *mturquoise_001.xml*), and every data reference file can store datasets that can be used for analysis (here *mTurquoise_dataset*). The *Models* folder includes model files (*mTurq_model.xml*) that are used in the Analysis scheme (*Analysis.xml*), stored under the *Analysis schema* folder

Trace plot. Changes to the selected time window can be applied by clicking the "Select time" button in the toolbar at the top of the Data tab.

4. For Glotaran data analysis, one should first create a new dataset from a data reference file (*see* **Note 8**). This can be done by clicking on the "create dataset" button in the toolbar of the data displayer and specify a name for the new dataset. The dataset will be created under the data reference file node (*see* Fig. 1). In principle it is possible to select all pixels and analyze the whole image, but in most cases, it is more appropriate to just select pixels of interest (*see* **Note 9**). Pixels can be selected by either clicking on the pixels in the fluorescence intensity image or by specifying a threshold value. If the photon counts per pixel are low, there is an option to perform pixel binning by pressing the button "Binning" (*see* **Note 10**).

3.5 Setting Up an Analysis Scheme

All information necessary for analysis (which datasets are selected, which model to use, etc.) is stored in the analysis scheme file, which is enclosed within the project's "Analysis schema" folder (*see* Fig. 1). When a new project is created using the Empty Project template, it will already contain one empty analysis scheme in the "Analysis schema" folder as well as an empty model file in the folder "Models."

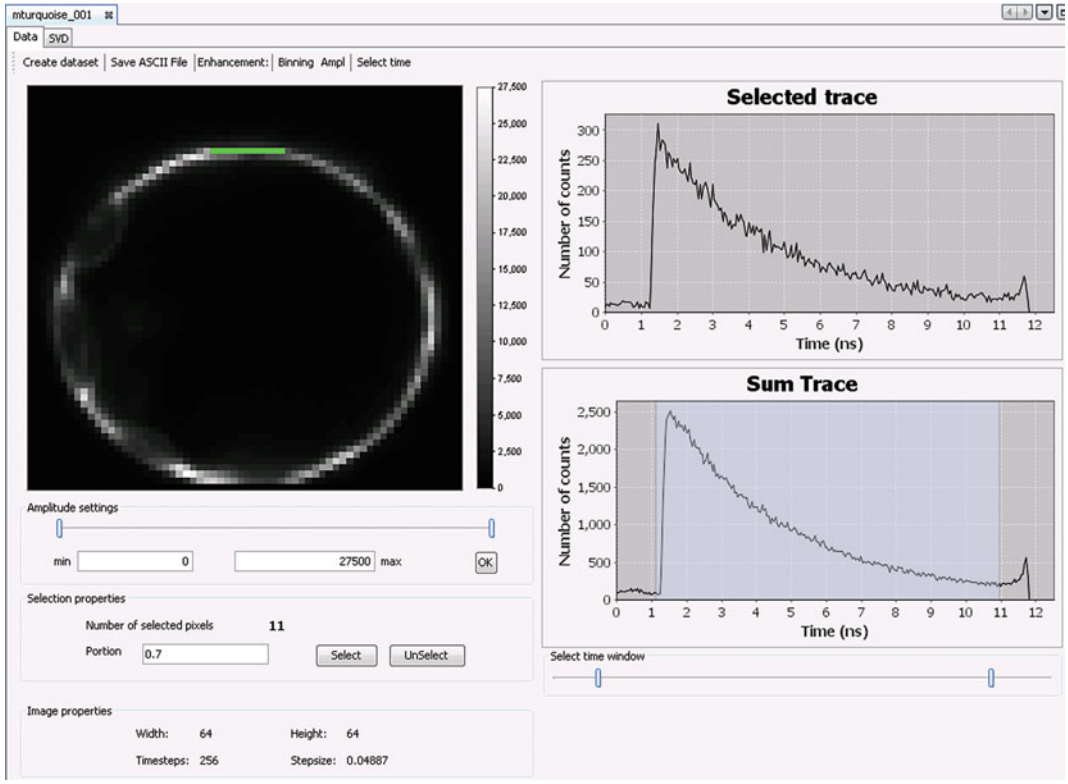

Fig. 2 Screenshot showing the Data tab of the FLIM data displayer displaying a data reference file or a dataset. Shown here is a fluorescence intensity image of a protoplast expressing mTurquoise1 acquired using the B&H 730 module. A description of the various components of the FLIM data displayer is given in Subheading 3.4, **step 3**

The first step in performing global analysis on a new dataset is typically to make an estimate of the number n_{comp} of distinct kinetic components underlying the data. In FLIM analysis this is estimating the number of unique fluorescence components present in the data. The singular value decomposition of the data matrix (SVD) can be a powerful tool to make the initial estimate (*see* **Note 11**) and is available directly from the data displayer window.

1. By clicking on "SVD" tab in the data displayer window (Fig. 2), the SVD of the corresponding dataset will be automatically calculated. Figure 3 shows the SVD of the *mTurquoise1_001* dataset for the first three SVD components. In this example, we can observe two distinct fluorescence components: one relatively slow component with a high contribution (first singular vector) and one very fast component with a lower contribution (second singular vector). Both processes should be taken into account when defining the starting model for analysis. Note that the third singular vector cannot be distinguished from the noise.

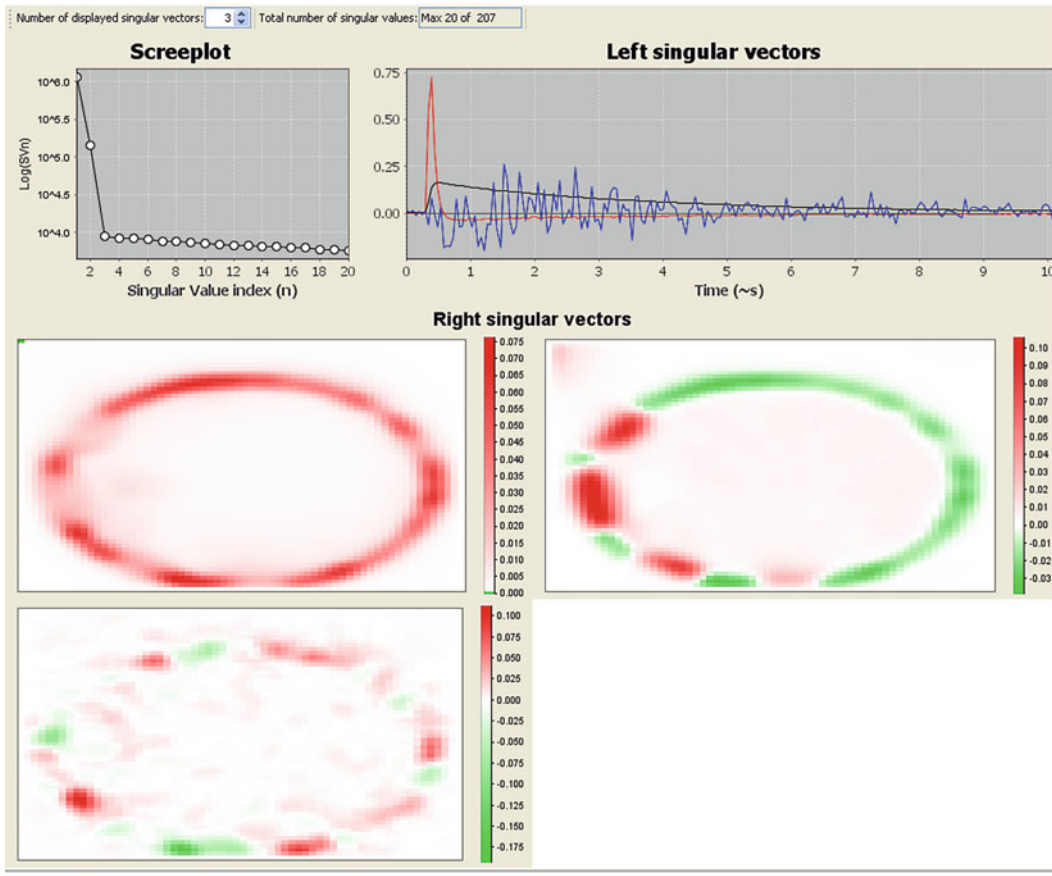

Fig. 3 SVD decomposition of a fluorescence intensity image of a protoplast expressing mTurquoise1. The *top right panel* shows the first three left singular vectors (LSV) (in time), the *bottom panel* shows the corresponding right singular vectors (RSV) (spatial), and, finally, the *top left panel* shows the screeplot of the first 20 singular values. Looking at the LSV suggests the presence of at least two linearly independent components (one slow, *black line*, and one fast, *red line*) significantly different from noise, whereas the third component (*blue line*) is likely due to noise. The RSV depicts the spatial distribution of independent components, showing a few regions with more pronounced fast component

2. *Double click* on the analysis scheme file (Analysis.xml in Fig. 1) to open the analysis scheme editor window, which allows setting up all relevant parameters necessary for analysis (*see* **Note 12**). Figure 4 shows the analysis scheme that was used to analyze a single dataset *mTurquoise_dataset* (*see* **Note 13**).
3. As observed from the SVD analysis, there are at least two distinct kinetic components underlying the data from this experiment. One of these components can likely be attributed to autofluorescence from the chloroplasts and the other to mTurquoise1 fluorescence. The fluorescence decay of mTurquoise1 is modeled using a kinetic parameter shown as "KinPar" in the model with one rate parameter (*see* **Note 14**).

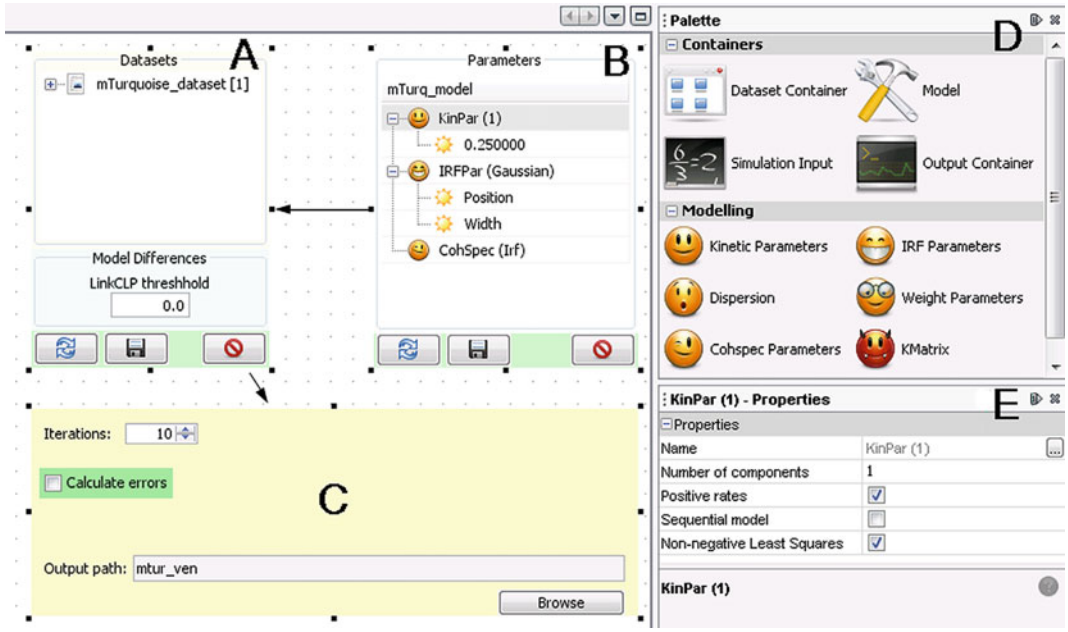

Fig. 4 Screenshot of the analysis scheme editor windows and associated palette and properties windows. On the analysis scheme editor canvas, the following containers are shown: (**a**) *Dataset container*, which contains a list of datasets that will be analyzed (*see* **Note 16**); (**b**) *Model container*, which includes relevant model parameters used in analysis; and (**c**) *Output container*, which is used to specify the name of the folder where the result files will be written (*see* **Note 17**) and specifies the maximum number of iterations used in the optimization algorithm by the underlying software (*see* **Note 18**). The *right side* of the screenshot contains (**d**) the *Palette*, which contains various containers that can be dragged onto the canvas and modeling nodes can be dragged into the *Model container*, and (**e**) the *Properties* window allows for editing of the properties of the selected node (in this example, the kinetic parameters node (KinPar) from the *Model Container* is selected)

The starting value for the decay rate ($1/\tau$) is given in the name of the subnode and can be adjusted using the properties window (Fig. 4e). In this example, the autofluorescence component is modeled by a parameter "CohSpec." This option can be used to account for all processes that occur in parallel to any normal decay process and which rise and decay within the time duration of the instrument response function (IRF) of the measurement setup, such as autofluorescence or scattering. This process, which is typically modeled as having the time profile of the IRF, can be subtracted from the data prior to estimating the real kinetic components of donor and/or acceptor. In the present study, the FLIM setup has a time resolution of around 120 ps, which makes it impossible to resolve the autofluorescence component, and therefore the "CohSpec" option is used to account for this effect (*see* **Note 15**).

4. The final element to add to the model container in the analysis scheme is the "IRFPar" option. This node contains all relevant parameters to model the IRF of the experiment. Typically,

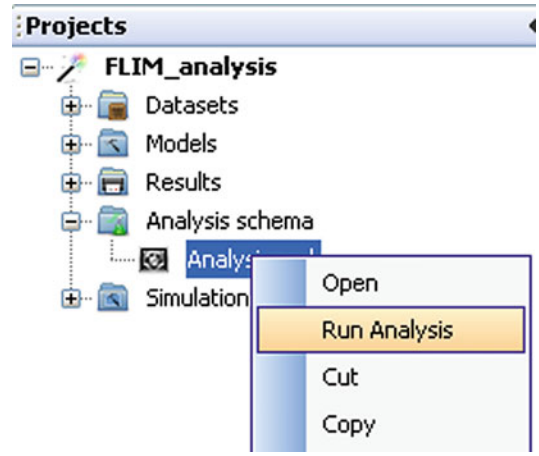

Fig. 5 Screenshot of the project window, displaying "Run analysis" command

in FLIM measurements the IRF cannot be represented by an analytical function, such as a Gaussian. Therefore, in many cases the IRF is measured and numerically convolved with the exponential decay model (*see* **Note 16**). Nevertheless, the time resolution of this particular experiment (*see* **Note 15**) is such that it is possible to approximate the IRF with a Gaussian to obtain reliable fits. For this analysis, the IRF is approximated using a Gaussian function depending on the parameters μ and Δ, being the temporal position of the maximum and the full width at half maximum (FWHM) respectively:

$$\mathrm{IRF}(t) = \frac{1}{\tilde{\Delta}\sqrt{2\pi}} \exp\left(-\log(2) \left(\frac{2(t-\mu)}{\Delta} \right)^2 \right), \qquad (5)$$

where $\tilde{\Delta} = \Delta / \left(2\sqrt{2\log(2)}\right)$.

Reasonable starting values for the parameters μ and Δ should be provided, which are then optimized during the analysis. In principle, μ and Δ are free parameters, although they can be fixed, if they can be determined more accurately by other means.

5. In the output container, a specific folder name is created in which the analysis results are saved to. The analysis results will be stored in this folder under the "Results" folder in the project (*see* Fig. 5). If a results folder already exists (for instance, when the analysis is rerun a second time, without specifying a different name), a number will be appended to the name of the folder.
6. Also in the output container the maximum number of iterations can be specified, for which the software should optimize the nonlinear parameters of the model (such as the rate constants and IRF parameters). The conditionally linear parameters

(the amplitudes of every component per pixel) are always optimized, even at 0 iterations. Usually one starts any modeling process with a sanity test by specifying 0 iterations to test the validity of the initial starting parameters. If the starting values are found to be reasonable, the number of iterations can be increased to, for instance, 5 or 10 (*see* **Note 17**).

7. After setting up the complete analysis scheme correctly, the file can be executed to start global analysis of the data. To do this, select the "Run Analysis" option from the context menu of the analysis scheme file by right clicking on the file (*see* Fig. 5). After this, a progress indicator in the bottom right part of the software window will show that the analysis is running.

3.6 Validating Analysis Results

1. When the analysis is complete, the results will appear in the specified folder under the "Results" folder in the project folder (*see* **Note 18**). The results of the analysis of the mTurquoise1 dataset are shown in Fig. 6.
2. Figure 6 shows the estimated fluorescence lifetimes, corresponding error, the fluorescence intensity map, and corresponding color-coded average fluorescence lifetime image as well as a distribution of the average fluorescence lifetime (*see* **Note 19**). Here, a single number for the average fluorescence lifetime (3.6 ns) is shown, because a mono-exponential model is used for analysis. The lack of structure in the SVD of the residual matrix is a good indicator for the quality of the fit.

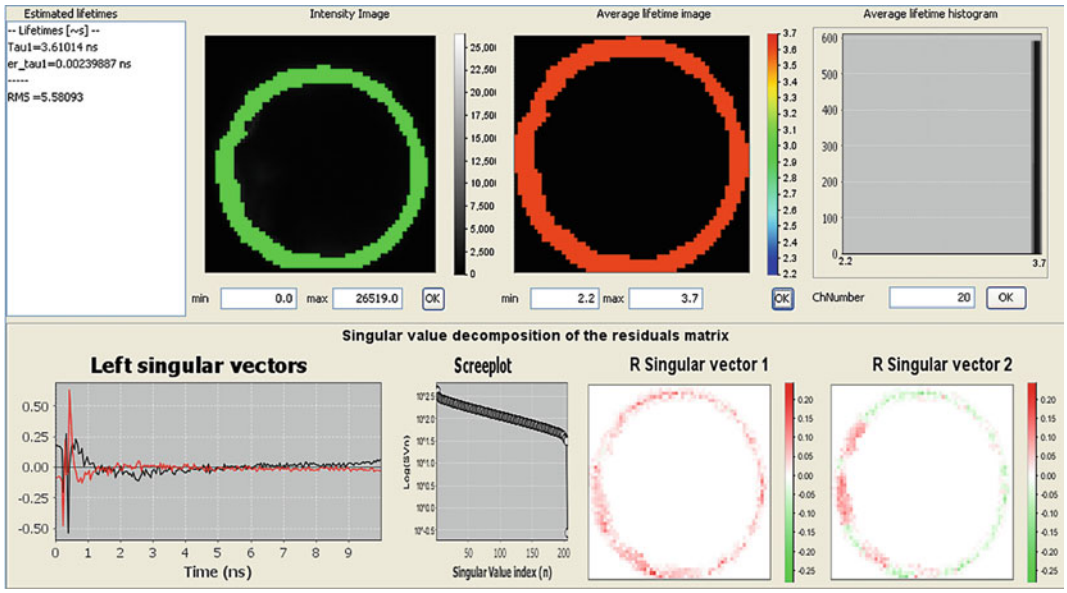

Fig. 6 FLIM results displayer giving an overview of the results of the analysis

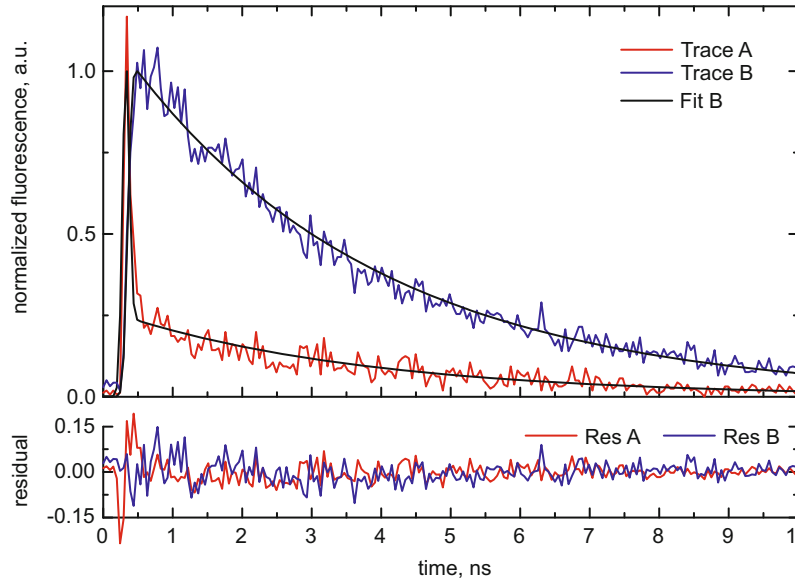

Fig. 7 Two fluorescence decay traces and fits from pixels with (Trace A, *red*) and without (Trace B, *blue*) autofluorescence. Weighted residuals are presented in the *bottom panel*

3. The results in Fig. 6 show that fluorescence of the protoplasts transfected with the mTurquoise1 displays a mono-exponential decay with a lifetime of 3.6 ns in plant cells, which is in agreement with studies performed in mammalian cells as well as in vitro experiments [16, 17]. Figure 7 shows fluorescence decay traces from two selected pixels with and without a pronounced autofluorescent component. The fitted trace and residuals obtained during global analysis shows good overlap with the raw data in both cases, which serves as justification of the relevance using the "CohSpec" parameter for compensating autofluorescence.

3.7 Analysis of mTurquoise1–mVenus Dataset

1. To analyze time-resolved fluorescence of mTurquoise1–mVenus fusion protein expressed in protoplasts, it is necessary to use a bi-exponential decay model (i.e., two rate constants) (*see* **Note 20**).
2. The average fluorescence lifetime image of the mTurquoise1–mVenus protein, shown in Fig. 8a, has an identical color scale as for mTurquoise1 alone. Comparing the average fluorescence lifetime of mTurquoise1 with the one of the mTurquoise1 fusion protein, it becomes clear that the presence of mVenus results in a reduction of the fluorescence lifetime of mTurquoise1 indicated by the change of color (from red to blue/cyan). This decrease can also be observed from time traces of selected pixels in Fig. 9.

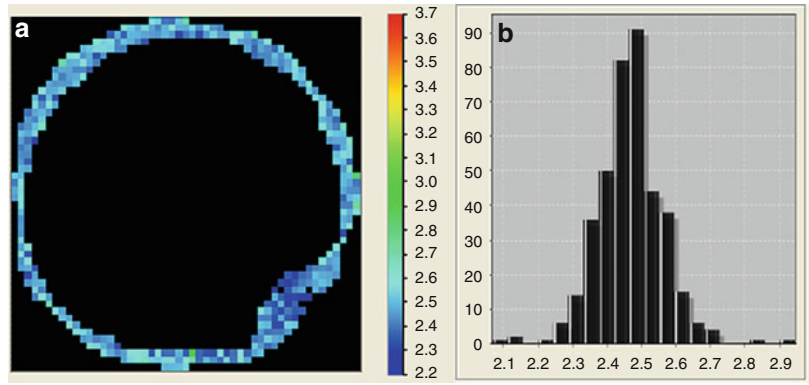

Fig. 8 Results of the analysis of the protoplasts transfected with mTurquoise1–mVenus using a bi-exponential decay model. (**a**) Average lifetime image. (**b**) Average lifetime histogram

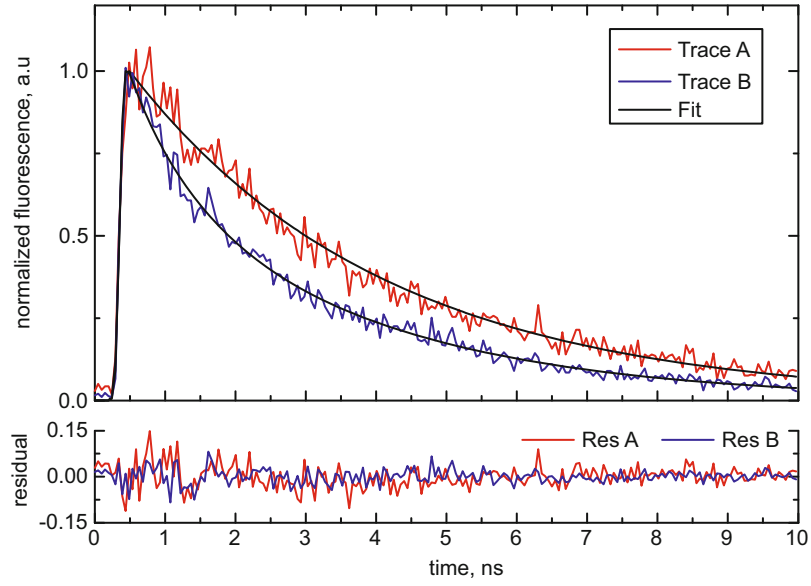

Fig. 9 Comparison of experimental and fitted fluorescence decay traces of mTurquoise1 alone (Trace A, *red*) and mTurquoise1–mVenus (Trace B, *blue*). Weighted residuals belonging to each fitted curve are presented in the *bottom panel*

3. Despite the clear decrease of the donor average fluorescence lifetime of the mTurquoise1–mVenus sample due to energy transfer, it remains difficult to quantify the FRET process. To improve analysis, one needs to analyze the estimated lifetime components and distributions of the corresponding

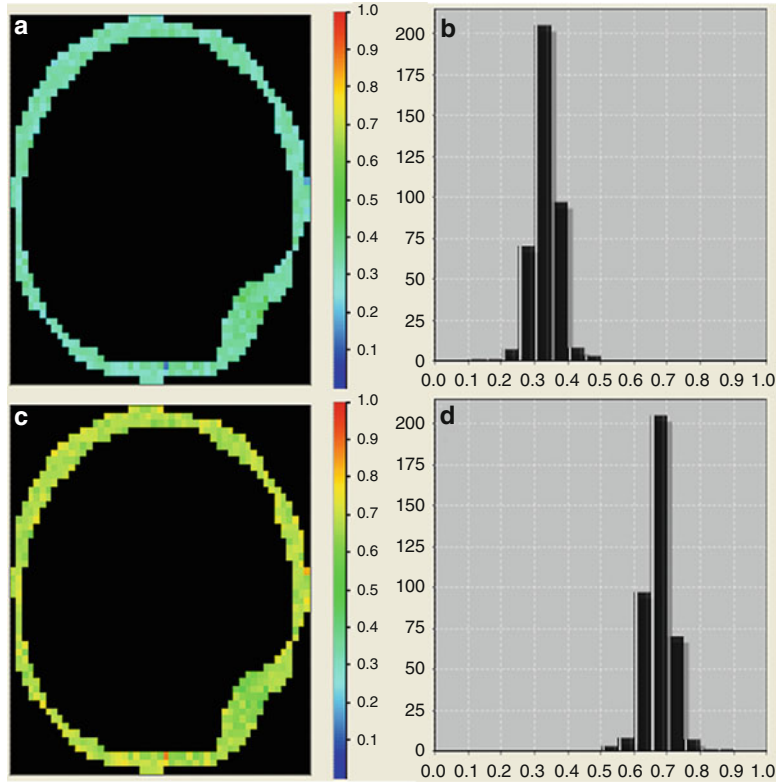

Fig. 10 Estimated distributions of the two estimated components. Here, (**a**) is the spatial distribution and (**b**) is the histogram of fractional distribution of component with fluorescence lifetime of 0.83 ns. And (**c**) is the spatial distribution and (**d**) is the histogram of fractional distribution of component with fluorescence lifetime of 3.3 ns

amplitudes. In the presented case, the estimated lifetimes are 0.83 ns with average amplitude around 35 % and 3.3 ns with average amplitude of 65 % (Fig. 10).

The long lifetime component (3.3 ns) is almost identical to the fluorescence lifetime of mTurquoise1 alone (3.6 ns) and can be attributed to "non-FRETting" mTurquoise1 molecules of the FRET sample (*see* **Note 21**). Because mTurquoise1 follows mono-exponential decay kinetics, the fast component of 0.83 ns of the FRET sample can be attributed to the donor molecules undergoing energy transfer from mTurquoise1 to mVenus. It is important to realize that, if one is interested in FRET efficiency quantification or distance calculation, the short component instead of the average fluorescence lifetime must be used. However, describing a whole population, one should take into account the relative contributions of the different components (*see* **Note 22**).

This type of analysis would be very difficult in case of using bi-exponential decaying donor molecules, since it will require more complicated models using three or even four exponential terms [11, 18]. The use of donor molecules that exhibit a mono-exponential fluorescence decay significantly simplifies quantitative analysis of FRET data.

4 Notes

1. The isolation of the protoplast from the leaves is carried out according to the Tape sandwich method described in ref. 19.
2. The B&H card only operates in combination with the Detector Controller Card (DCC) card.
3. The image size in both case studies was 15 × 15 μm. In order to have sufficient photon counts per pixel, the pixel size was set to 64 × 64 pixels resulting in a pixel size of ca 350 nm.
4. The fusion proteins could be observed both in the cytoplasm and the nucleus of the plant cell.
5. Installers for Linux, Mac OS X, and Windows operating systems are available and can be downloaded from http://glotaran.org/downloads.html. Documentation about the installation protocol can be found at: http://glotaran.org/wiki.html. A video demonstration can be found here: http://glotaran.org/demonstration.html.
6. To add a new dataset to the project, *right mouse click* on the "Datasets" folder or a subfolder and select "Open dataset file." In the resulting Open file dialog, select the respective file to be added to the project. Using the CTRL + *left mouse click* combination in the Open file dialog, more data files can be added simultaneously. After opening the data file(s), a data reference file is created and added to the project. The data reference file in the project folder only contains a reference or link to the actual data file. To store the actual data file inside the project folder, *right mouse click* the data reference file and select "Cache dataset to project folder." In this way the entire project can be copied onto a different computer for analysis. To organize the data reference files, more folders can be created in the Datasets folder.
7. The grey scale of the fluorescence intensity can be adjusted using the slider or by filling in the numbers in the amplitude settings box.
8. When a data file is opened in Glotaran, a data reference file is created in the Datasets folder within the project. The data reference file only contains a link to the actual data file to protect the user accidentally modifying the original data during

preprocessing of the data. Therefore, before starting the analysis on any kind of data file, first, a new dataset should be created from the data file.

9. Selection of pixels for analysis is performed for several reasons. First, analysis of pixels containing only fluorescence of donor molecules or molecules of interest significantly decreases computation time. Second, it allows excluding those pixels with pronounced, undesirable (auto)fluorescent components from the analysis. In this way the number of required parameters for the analysis can be minimized, and the accuracy by which these parameters can be estimated improved.
10. In case the number of photons is too low for quantitative analysis, a binning factor can be used. Binning is a procedure where the selected pixel is analyzed, but the neighboring pixels are included for calculation of the fluorescence lifetime. The binning factor can be calculated according to the following formula: binning factor $= (2n + 1)^2$, where n is number of pixels.
11. The singular value decomposition (SVD) is a model-free matrix factorization technique, which decomposes the data into a sum of orthonormal vector products scaled by singular values. Here, the left singular vectors (LSV) represent time dimension and the right singular vector (RSV) represents spatial dimension. The contribution to the data is the product of the nth left singular vector and right singular vector scaled by the nth singular value. The singular vectors are ordered based on their contribution to the data as represented by the magnitude of the corresponding singular values as shown in the screeplot [20, 21]. The technique can be used to explore the number of spectrally and spatially independent components in the data matrix, which is an important aspect of defining an initial model. However, it should be noted that an independent component in the SVD analysis does not necessarily represent a single lifetime component [22].
12. A functional analysis scheme should have three connected containers, one *model container* linked to one *dataset container*, linked to one *output container*. To create the *dataset container* and *output container*, drag and drop the corresponding icons from the palette (Menu: Window—Palette), which is available on the right of the analysis scheme editor (Fig. 4d), to the canvas. The *model container* can be created either from an existing model file, by dragging the model file from the *Models* folder in the project manager to the canvas, or from the palette, by dragging the Model icon from the palette to the canvas, thus creating a new model file which will be added to the Models folder in the project. Finally, the model container should be

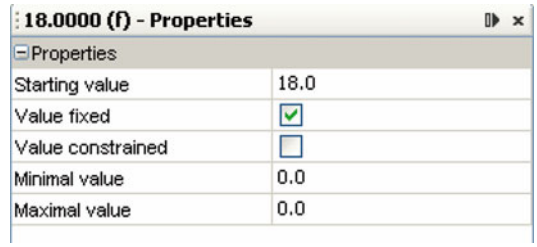

Fig. 11 Example property window of a parameter node

connected to the dataset container, and the dataset container should be connected to the output container. To connect two containers, press and hold the Ctrl (Windows, Linux) or Cmd+CTRL (Mac)key, click the top of a container, and drag the connector arrow that appears from one container to another.

13. To add datasets to the dataset container, drag and drop them from the project manager. By default, all added datasets would be placed in the same group (number in the square brackets next to the dataset name). For all datasets from the same group, the amplitudes will be linked. For simultaneous analysis of multiple FLIM images, all datasets have to be in the separate groups. It is possible to change the group assigned to the dataset in the properties of the dataset (right click menu or Properties window) (Fig. 5e).
14. To add different parameters to the model, drag the corresponding icon from the palette (Fig. 5d). Each parameter has its own properties that can be edited from the property window (Fig. 5e). The property window in Fig. 5 represents the property of the kinetic parameters. The number of components property defines the number of rates (or reciprocal lifetimes) that will be fitted. The positive rates property will constrain rates to be positive (for FLIM analysis, it is always true), and the nonnegative least-squares property will force amplitudes of the component to be positive (in most cases of FLIM analysis, this is also true; however, in case of analyzing rise times of the fluorescence [11], that property should be set to false). When the number of kinetic parameters is set, the node for each kinetic parameter will be created as a subnode for "KinPar" node. Figure 11 represents a property window corresponding to the parameter node. In this property, the starting value for the parameter that will be used for analysis should be set. The parameter can be fixed or constrained by setting minimal and maximal values.
15. The time channel spacing in the present study is 48 ps/channel. The excitation source, the photodetector, and associated electronics define the FWHM of the IRF. A femtosecond laser,

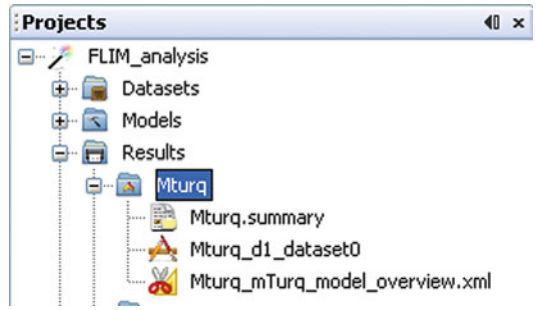

Fig. 12 Screenshot of the project manager window showing the generated result files

together with the used single-photon counting detection system, makes the FWHM of the IRF in the present experiments in the order of 120 ps. With the given signal-to-noise ratio (SNR), processes that are faster than 120 ps are not possible to estimate during analysis. Therefore, we can use the "CohSpec" option to compensate for an autofluorescence component. In experiments with higher time resolution [23], such modeling of the autofluorescence would be impossible, and one would need to use additional kinetic parameter(s) to account for the contribution of autofluorescence.

16. Various algorithms for numerical convolution of an exponential decay with a measured IRF can be applied. The iterative reference and scatter methods described in [24–26] perform well in practice and are implemented in Glotaran. The reference convolution method uses a measured fluorescence decay of a reference compound with a well-defined mono-exponential decay in a convolution procedure. This allows measuring the IRF of the setup exactly under the same conditions as the experiment, as well as estimate an IRF in multi-photon excitation systems. This is in sharp contrast when using a scattering solution to obtain the IRF, because one would need to change the detection wavelength.
17. Valid starting values are found if the analysis returns results at 0 iterations (i.e., the analysis does not crash and returns no valid results at all). However, this does not imply that the starting values are reasonable. The analysis is especially sensitive to the IRF parameters starting values.
18. An analysis progress indicator in the lower right corner of the window will indicate the progress of the data analysis. If the analysis is finished, three files will be created in the results folder (*see* Fig. 12). The file with extension "summary" provides a textual summary of the data analysis. Given are the final residual standard error and values of the fitted parameters with their standard errors, the number of iterations for the analysis,

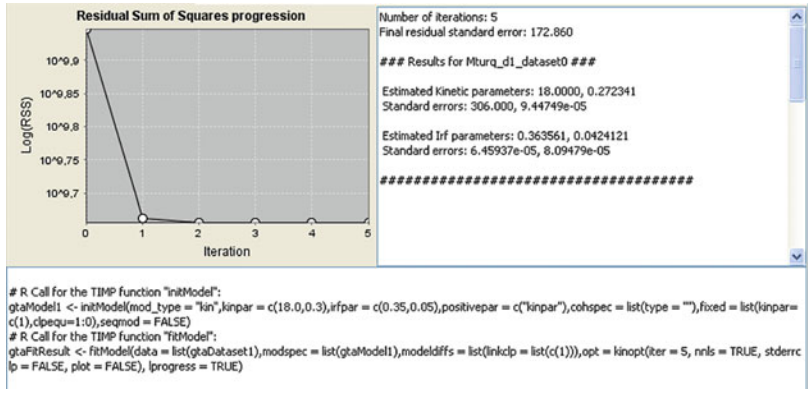

Fig. 13 Screenshot of the "Overview" file windows showing the residual sum of squares progression plot, the estimated parameters of the analysis with corresponding errors, and the calls made to the R package TIMP [15, 27] to perform the analysis

and the function calls that were made to the R package TIMP [15, 27] in order to perform that analysis. If the analysis failed, because of a wrong model or the initial guess for the parameters is too far off, then this file will be the only generated file, and it will contain a diagnostic error message rather than the parameters. The file with the name ending with "overview" shows a graphical view of the progress of the residual sum of squared errors. This graph will appear, if the fit was converged. Here, there was no progress in the last iterations from 2 to 5 (Fig. 13). This is an important criterion, because before convergence it is not possible to judge the quality of the model. The last generated file contains the results of the fit for a dataset. In case of simultaneous analysis of multiple datasets, there will be a file for each analyzed dataset.

19. The average fluorescence lifetime is calculated with the formula $\langle\tau\rangle = \sum_i \alpha_i \tau_i$ where τ_i is the lifetime of ith component and α_i is its amplitude such that $\sum_i \alpha_i = 1$.
20. The SVD analysis of the mTurquoise1–mVenus dataset indicates the presence of at least two independent components; one of them can be attributed to autofluorescence and the other to fluorescence from mTurquoise1. However, using a mono-exponential model including a "CohSpec" parameter (as it was used in donor only case) does not describe the data correctly. Figure 14 shows the left singular vector of the residuals after single- and bi-exponential analysis. The single-exponential analysis has clear systematic bias in the shape, which is an indication for a misfit of the data.
21. In principle, the "non-FRETting" donor molecules should have a similar fluorescence lifetime as the donor only sample. However, in the fusion protein the local environment of the

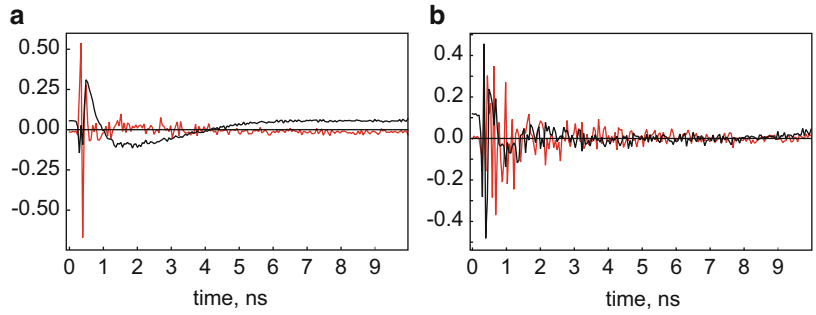

Fig. 14 First two left singular vectors obtained after the analysis of mTurquoise1–mVenus dataset using a mono-exponential (**a**) and a bi-exponential model (**b**)

Table 1
Summarized estimates of FRET efficiency and donor–acceptor distance using the average fluorescence lifetime or the shorter lifetime of the estimated FRET component

	Using lifetime of the estimated component involved in FRET	Using the average fluorescence lifetime
Estimated efficiency (%)	75	25
Estimated distance (nm)	4.2	6.2

The fluorescence lifetime of donor only is 3.6 ns and used for calculation of FRET efficiency (*see* Eq. 4). Using the lifetime of 3.3 ns estimated as "non-FRETting" population of the donor in the FRET sample does not change the values significantly. A critical distance $R_0 = 5.4$ nm is used for distance calculations

donor might be slightly different because of the presence of the (acceptor) protein. Another reason for observing differences of donor lifetimes could be crosstalk of acceptor fluorescence in the donor detection channel. The fluorescence lifetime of mVenus is in the order of 3 ns, and therefore with the given time resolution and SNR, this component would be indistinguishable from the donor fluorescence lifetime. Thus, a mixture of acceptor fluorescence in the donor detection channel can potentially give rise to a different estimate of the donor fluorescence lifetime.

22. Using the average fluorescence lifetime to calculate FRET efficiencies and distances will result in an underestimation of the expected values. In the present study, the calculation of the FRET efficiency was compared using the average fluorescence lifetime and the estimated short lifetime (*see* Table 1). This underestimation of the parameters will depend on the amount of

"non-FRETting" donor molecules. There are several reasons for this population to be present in the data:

(a) Direct excitation of the acceptor molecules—if acceptor molecules are in the excited state, energy transfer from excited donor to acceptor molecules cannot take place.

(b) Photobleaching of the acceptor—irreversibly destroyed acceptor molecules cannot accept energy from excited donor molecules. Photobleaching can occur by direct excitation of the acceptor or by the energy transfer process.

(c) Photoconversion of acceptor molecules—many fluorescent proteins (FPs) that are used as acceptors can be photoconverted to a species of which the fluorescence properties are different from the original species [28].

(d) Protonation of fluorescent proteins may also change spectroscopic properties of the particular FP as has been observed for YFP (mVenus) [29].

(e) Differences in maturation time of the fluorescent proteins within the FRET pair can give a rise to a large population of "non-FRETting" donor molecules [11].

When studying protein–protein interactions with the FRET method in which FPs are fused to the proteins of interest, one should be careful with assignment of a noninteracting population. The presence of donor molecules not participating in FRET does not necessarily imply that the proteins of interest are not interacting, but interactions cannot be detected by FRET.

References

1. Borst JW, Visser AJWG (2010) Fluorescence lifetime imaging microscopy in life sciences. Meas Sci Technol 21:102002
2. Beechem JM (1992) Global analysis of biochemical and biophysical data. Methods Enzymol 210:37–54
3. Bednarkiewicz A, Whelan MP (2008) Global analysis of microscopic fluorescence lifetime images using spectral segmentation and a digital micromirror spatial illuminator. J Biomed Opt 13:041316
4. Barber P, Ameer-Beg S, Gilbey J et al (2009) Multiphoton time-domain fluorescence lifetime imaging microscopy: practical application to protein-protein interactions using global analysis. J R Soc Interface 6:S93–S105
5. Wlodarczyk J, Woehler A, Kobe F et al (2008) Analysis of FRET signals in the presence of free donors and acceptors. Biophys J 94: 986–1000
6. Laptenok SP, van Stokkum IHM, Borst JW et al (2012) Disentangling picosecond events that complicate the quantitative use of the calcium sensor YC3.60. J Phys Chem B 116: 3013–3020
7. Snellenburg JJ, Laptenok SP, Seger R et al (2012) Glotaran: a Java-based graphical user interface for the R-package TIMP. J Stat Softw 49(3):1–23
8. Bücherl C, Aker J, de Vries S et al (2010) Probing protein-protein Interactions with FRET-FLIM. Methods Mol Biol 655:389–399
9. Russinova E, Borst JW, Kwaaitaal M et al (2004) Heterodimerization and endocytosis of Arabidopsis brassinosteroid receptors BRI1 and AtSERK3 (BAK1). Plant Cell 16: 3216–3229
10. Verveer PJ, Squire A, Bastiaens PIH (2000) Global analysis of fluorescence lifetime imaging microscopy data. Biophys J 78:2127–2137
11. Laptenok SP, Borst JW, Mullen KM et al (2010) Global analysis of Förster resonance energy transfer in live cells measured by fluorescence lifetime imaging microscopy

exploiting the rise time of acceptor fluorescence. Phys Chem Chem Phys 12:7593–7602
12. Valeur B (2002) Molecular fluorescence: principles and applications. Wiley-VCH, New York
13. Lakowicz JR (2006) Principles of fluorescence spectroscopy, 3rd edn. Springer, New York
14. Förster T (1949) Experimentelle und theoretische Untersuchung des zwischenmolekularen Ubergangs von Elektronenanregungsenergie. Z Naturforsch 4a:321–327
15. Laptenok SP, Mullen KM, Borst JW et al (2007) Fluorescence lifetime imaging microscopy (FLIM) data analysis with TIMP. J Stat Softw 18(8):1–20
16. Klarenbeek JB, Goedhart J, Hink MA et al (2011) A mTurquoise-based cAMP sensor for both FLIM and ratiometric read-out has improved dynamic range. PLoS One 6: e19170
17. Goedhart J, van Weeren L, Hink MA et al (2010) Bright cyan fluorescent protein variants identified by fluorescence lifetime screening. Nat Methods 7:137–139
18. Borst JW, Laptenok SP, Westphal AH et al (2008) Structural changes of yellow Cameleon domains observed by quantitative FRET analysis and polarized fluorescence correlation spectroscopy. Biophys J 95:5399–5411
19. Wu F-H, Shen S-C, Lee L-Y et al (2009) Tape-Arabidopsis sandwich—a simpler Arabidopsis protoplast isolation method. Plant Methods 5:16
20. Press WH, Teukolsky SA, Vetterling WT et al (2007) Numerical recipes: the art of scientific computing, 3rd edn. Cambridge University Press, Cambridge, MA
21. Golub GH, Van Loan CF (1996) Matrix computations, 3rd edn. The Johns Hopkins University Press, Baltimore, MD
22. Laptenok SP, Visser NV, Engel R et al (2011) A general approach for detecting folding intermediates from steady-state and time-resolved fluorescence of single-tryptophan-containing proteins. Biochemistry 50:3441–3450
23. Krumova SB, Laptenok SP, Borst JW et al (2010) Monitoring photosynthesis in individual cells of Synechocystis sp. PCC 6803 on a picosecond timescale. Biophys J 99:2006–2015
24. Grinvald A, Steinberg IZ (1974) Analysis of fluorescence decay kinetics by method of least-squares. Anal Biochem 59:583–598
25. Vos K, van Hoek A, Visser AJWG (1987) Application of a reference convolution method to tryptophan fluorescence in proteins. A refined description of rotational dynamics. Eur J Biochem 165:55–63
26. Boens N, Ameloot M, Yamazaki I et al (1988) On the use and the performance of the delta-function convolution method for the estimation of fluorescence decay parameters. Chem Phys 121:73–86
27. Mullen KM, van Stokkum IHM (2007) TIMP: an R package for modeling multi-way spectroscopic measurements. J Stat Softw 18(3):1–46
28. Kremers G-J, Hazelwood KL, Murphy CS et al (2009) Photoconversion in orange and red fluorescent proteins. Nat Methods 6:355–358
29. McAnaney TB, Zeng W, Doe CFE et al (2005) Protonation, photobleaching, and photoactivation of yellow fluorescent protein (YFP 10C): a unifying mechanism. Biochemistry 44: 5510–5524